Supplement of Nat. Hazards Earth Syst. Sci., 22, 2257–2287, 2022
https://doi.org/10.5194/nhess-22-2257-2022-supplement

Natural Hazards and Earth System Sciences
Open Access
EGU

Supplement of

Fault slip potential induced by fluid injection in the Matouying enhanced geothermal system (EGS) field, Tangshan seismic region, North China

Chengjun Feng et al.

Correspondence to: Chengjun Feng (feng2010618@aliyun.com)

Supplement

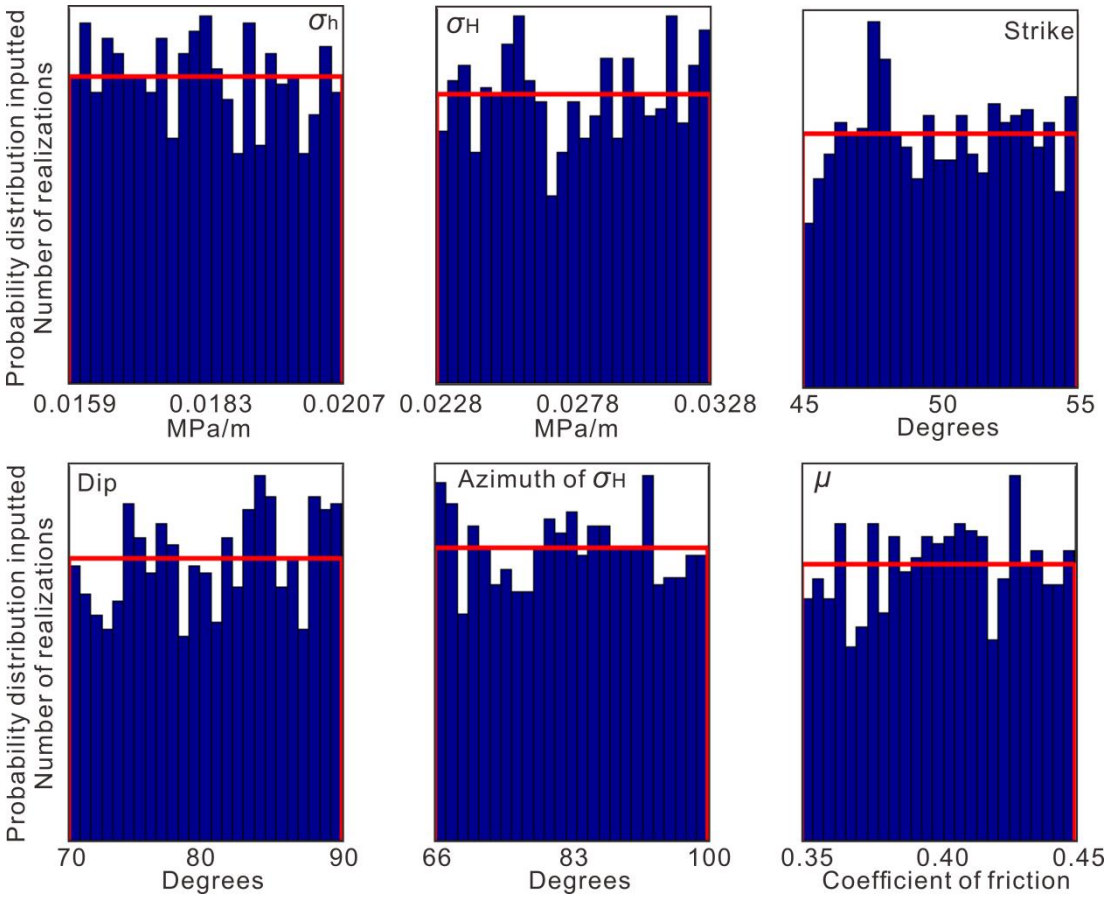

Figure S1. Probability distributions inputted of the initial in situ stress field and the characteristic parameters of the mapped fault $F_{4\text{-}1}$ of the Tangshan fault belt. σ_H and σ_h denote the maximum and minimum horizontal principal stresses, respectively.

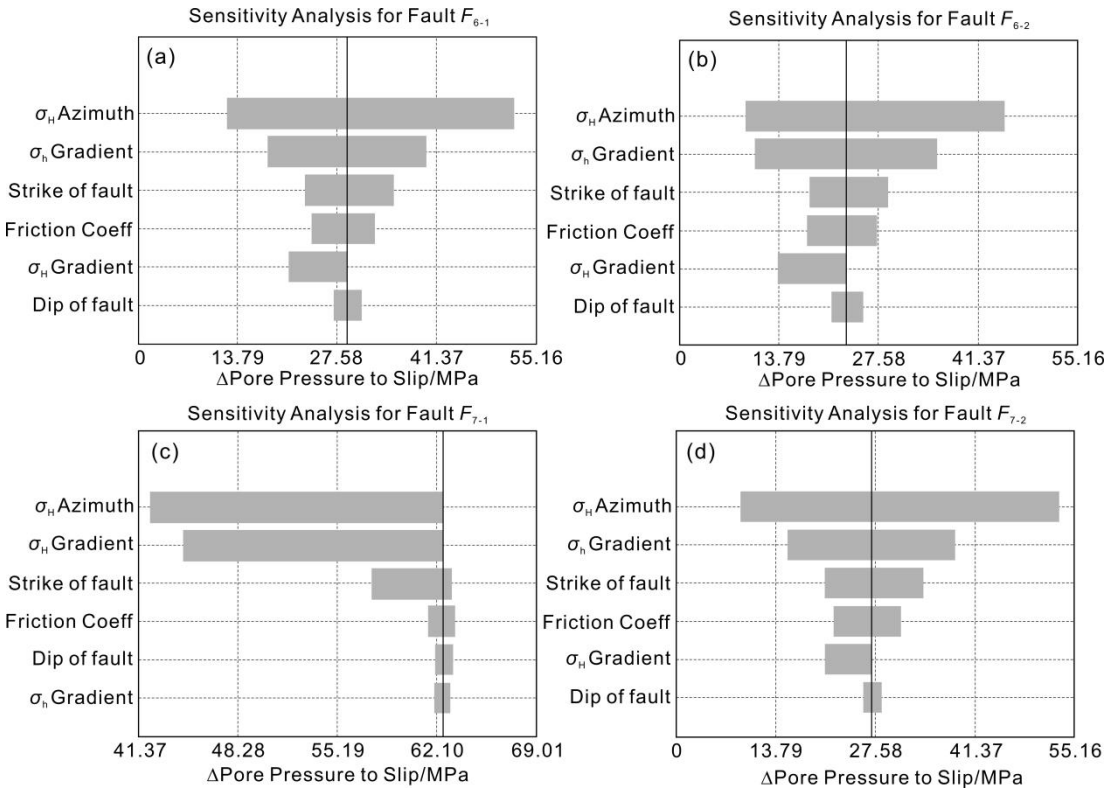

Figure S2. Sensitivity of the fault slip potential (FSP) on the mapped faults to uncertainties in various input parameters. **(a)** A case of fault F_{6-1}, **(b)** a case of fault F_{6-2}, **(c)** a case of fault F_{7-1}, and **(d)** a case of fault F_{7-2}.

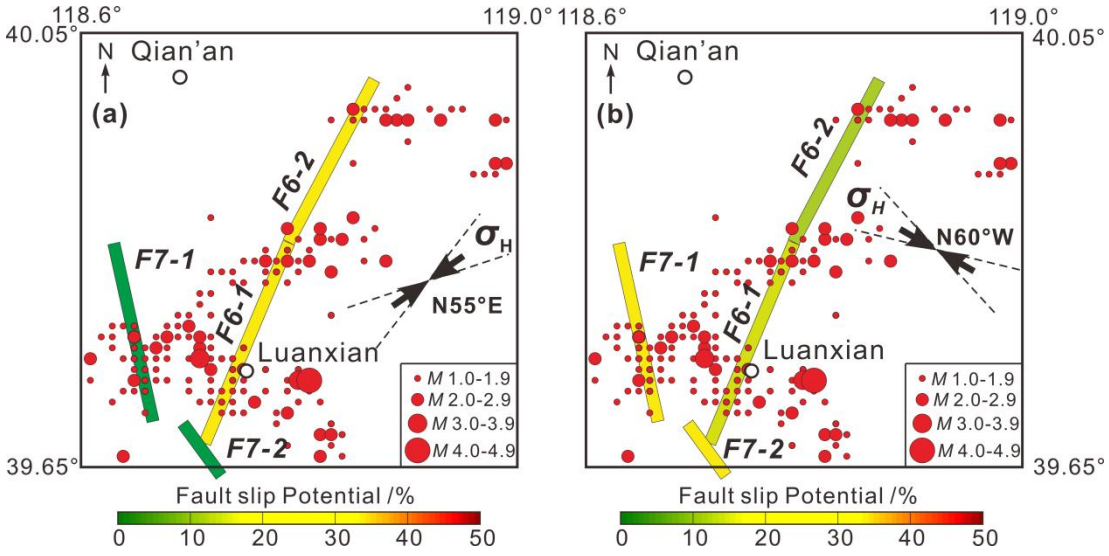

Figure S3. The probabilistic fault slip potential on the faults F_{6-1}, F_{6-2}, F_{7-1}, and F_{7-2} in Lulong basin and the σ_1 azimuth of the hypothetic local stress field. **(a)** The σ_1 is oriented at 55°±17°. **(b)** The σ_1 is oriented at 120°±17°.

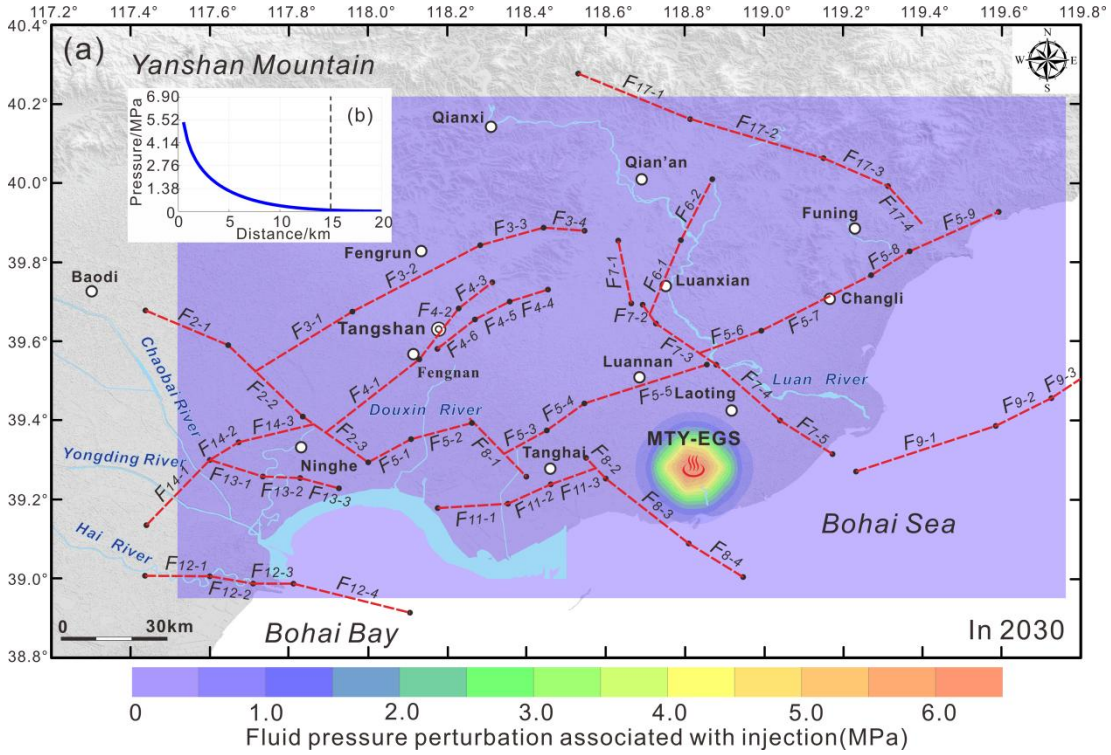

Figure S4. (a) Estimated fluid pressure perturbation in 2030 in response to fluid injection at five hypothetic wells in the MTY EGS field. **(b)** Estimated decay of the fluid pressure perturbation with distance in the MTY EGS field in 2030.

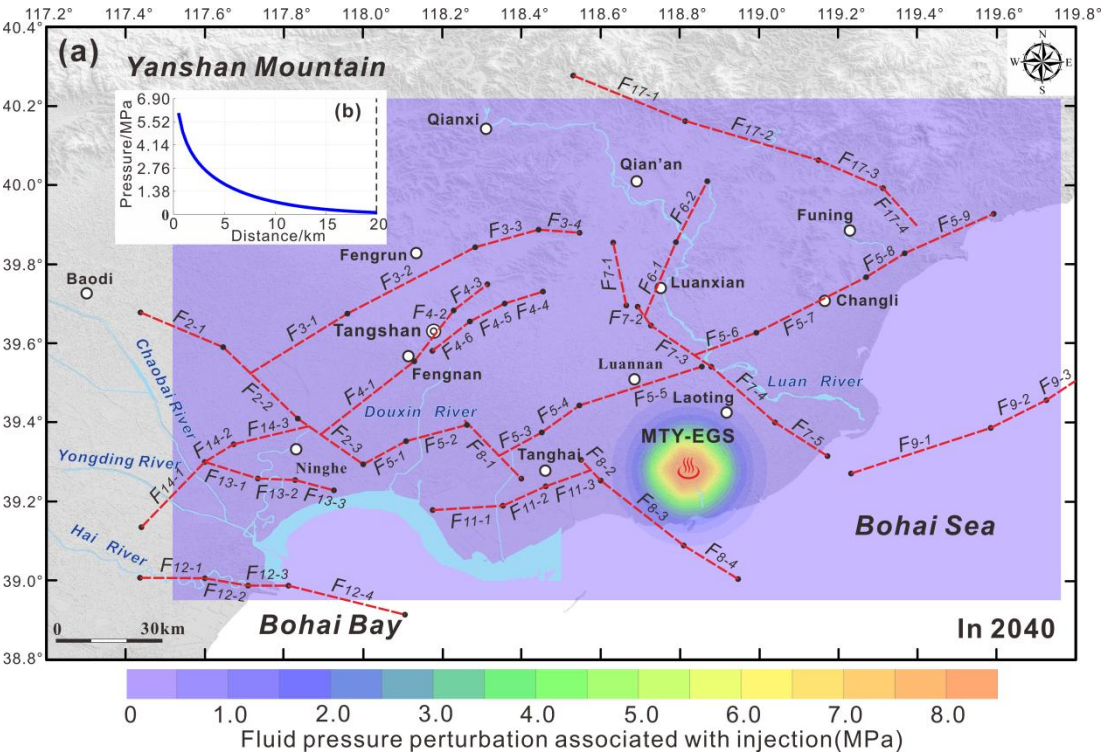

Figure S5. (a) Estimated fluid pressure perturbation in 2040 in response to fluid injection at five hypothetic wells in the MTY EGS field. **(b)** Estimated decay of the fluid pressure perturbation with distance in the MTY EGS field in 2040.

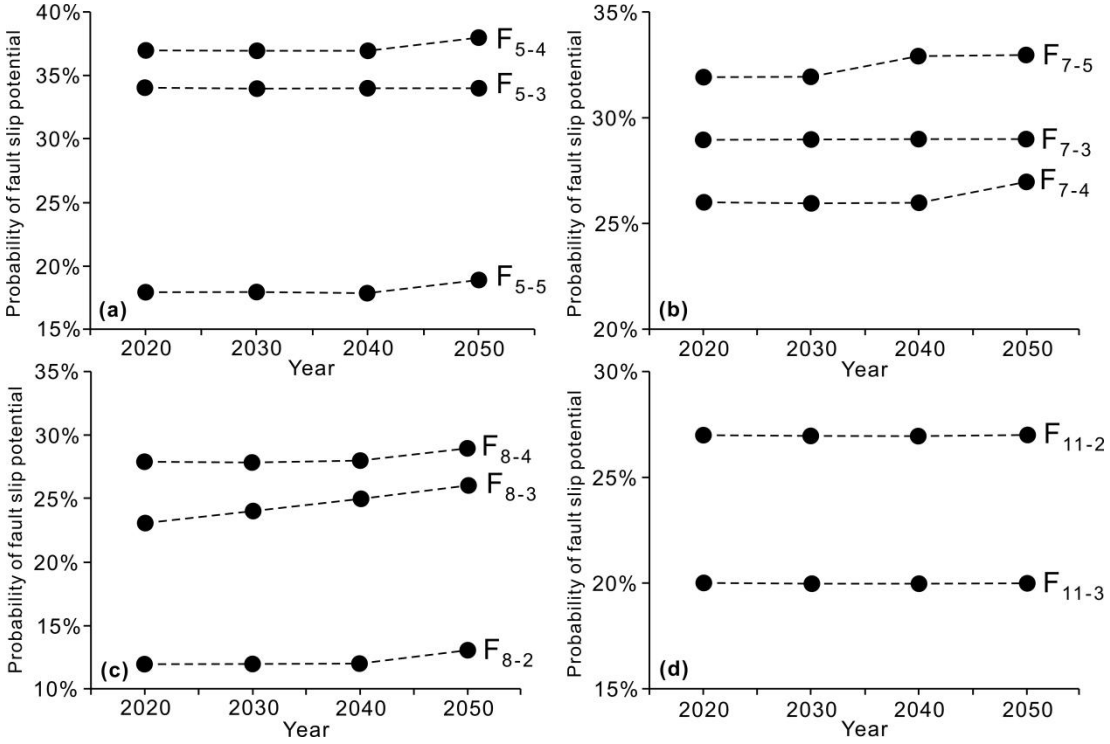

Figure S6. Changes of the probabilistic fault slip potential on the mapped faults within a range of ~30-45 km away from the injected wells in the MTY EGS field from 2020 to 2050. **(a)** The FSP values on the southwestern segment of the Changli-Ninghe fault. **(b)** The FSP values on the southeastern segment of the Luanxian-Laoting fault zone. **(c)** The FSP values on the Baigezhuang fault. **(d)** The FSP values on the Xi'nanzhuang fault.

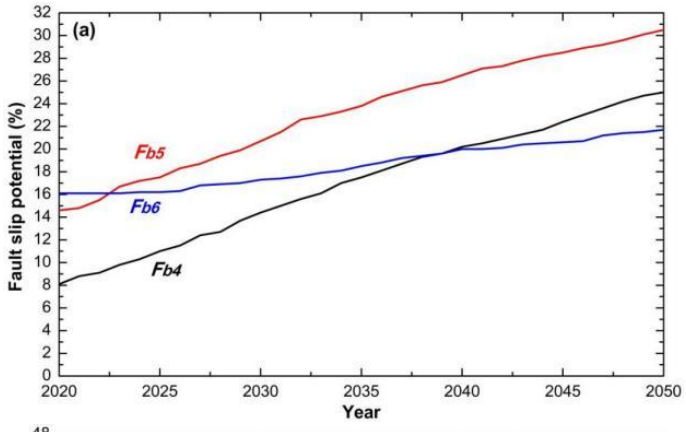
(a)
Fb5
Fb6
Fb4
Fault slip potential (%)
Year

1

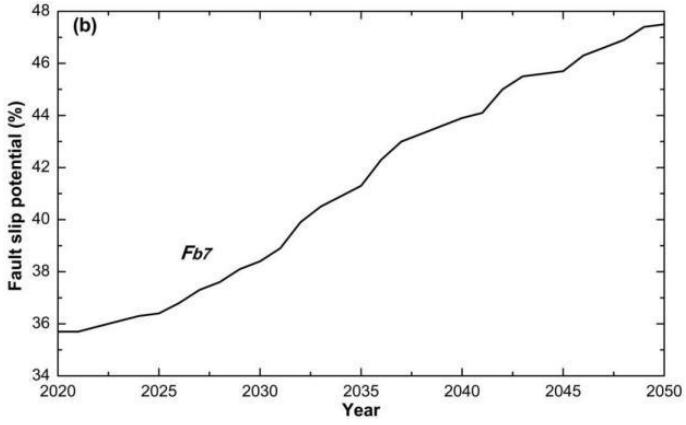
(b)
Fb7
Fault slip potential (%)
Year

2

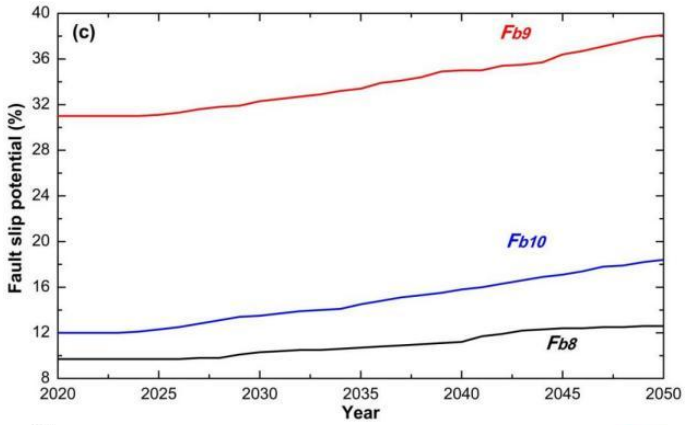
(c)
Fb9
Fb10
Fb8
Fault slip potential (%)
Year

3

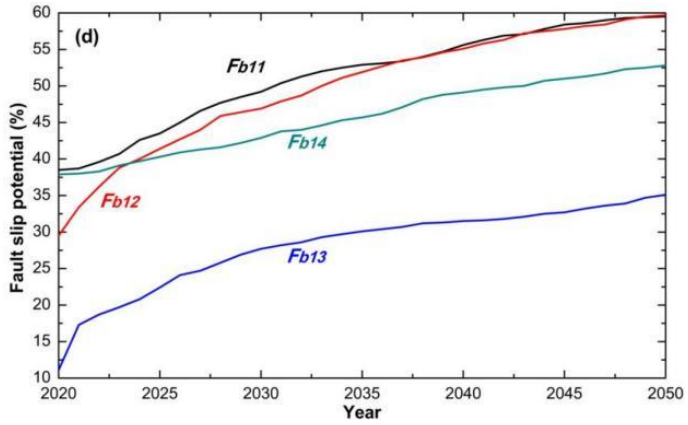
(d)
Fb11
Fb14
Fb12
Fb13
Fault slip potential (%)
Year

4

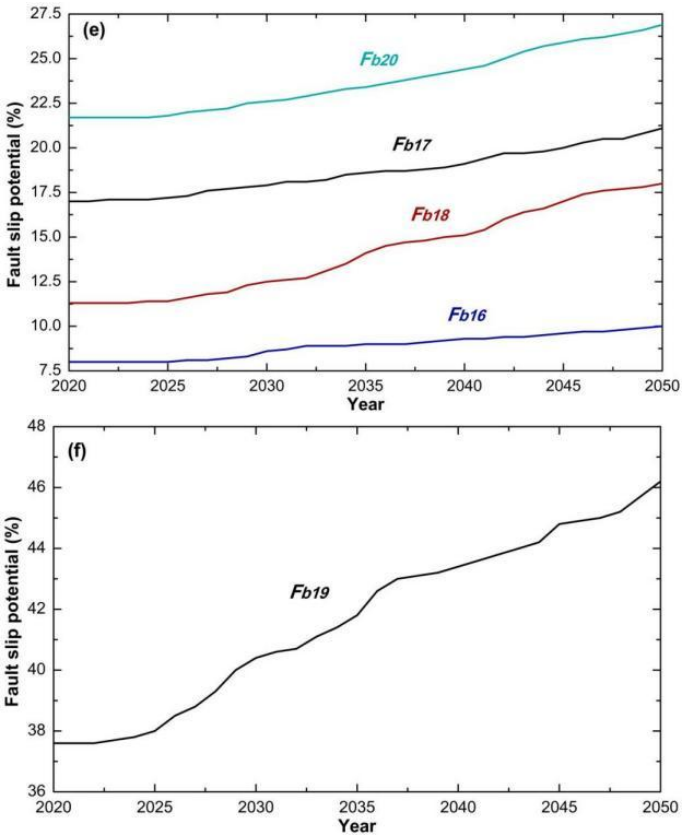

Figure S7. Changes of the probabilistic fault slip potential on the mapped faults within a range of ~15-20 km away from the injected wells in response to the hypothetic fluid injection in the MTY EGS field from 2020 to 2050.

1

2 **Table S1.** Focal mechanisms of small and moderate earthquakes in Tangshan seismic region, North China.

Number	Date	Longitude /(°E)	Latitude /(°E)	Depth /(m)	Magnitude	Strike I /(°)	Dip I /(°)	Rake I /(°)
1	2006.11.12	118.50	39.70	15	3.6	96	81	-42
2	2006.12.03	118.15	39.55	10	3.0	304	60	-6
3	2007.03.05	118.00	39.38	21	3.4	41	40	147
4	2007.09.04	118.73	39.73	10	3.4	112	82	-27
5	2007.11.17	119.13	39.58	19	3.5	171	86	-175
6	2007.12.27	118.08	39.50	10	3.3	192	42	-89
7	2008.03.11	118.90	39.98	15	4.3	105	56	61
8	2009.10.30	117.75	39.28	10	3.2	42	87	164
9	2009.11.22	117.78	39.45	14	3.7	308	66	-15
10	2010.01.28	118.88	39.97	12	2.7	215	85	85
11	2010.02.15	118.52	39.68	11	3.3	74	62	-49
12	2010.02.17	118.68	39.77	10	3.1	112	67	9
13	2010.03.06	118.48	39.68	11	3.8	302	56	53
14	2010.03.06	118.50	39.70	10	4.8	18	55	-84
15	2010.03.06	118.65	39.73	7	2.7	326	56	53
16	2010.03.06	118.48	39.68	11	2.6	215	45	-83
17	2010.03.06	118.50	39.70	10	3.6	278	57	33
18	2010.03.06	118.50	39.68	11	2.6	306	44	60
19	2010.03.06	118.48	39.68	11	3.2	300	67	46
20	2010.03.06	118.48	39.68	11	2.8	277	45	5
21	2010.03.07	118.52	39.68	6	3.2	92	71	-47
22	2010.03.07	118.50	39.68	11	2.7	241	57	-66
23	2010.03.22	118.45	39.77	11	3.0	298	56	-72
24	2010.04.09	118.07	39.47	12	4.6	340	87	-4

25	2010.04.09	118.07	39.48	12	3.1	320	64	79
26	2010.05.02	118.47	39.12	10	3.2	210	10	-90
27	2010.05.17	118.67	39.77	10	2.9	297	83	29
28	2010.06.21	118.88	39.97	4	3.1	134	64	16
29	2010.07.12	118.08	39.52	8	2.5	250	70	79
30	2010.7.22	118.62	39.77	3	2.6	341	70	-79
31	2010.08.09	118.75	39.73	5	2.6	278	56	-78
32	2010.09.05	118.62	39.75	10	2.8	121	85	-65
33	2010.09.11	118.83	39.87	7	2.7	127	51	-77
34	2010.09.20	118.50	39.78	3	2.6	338	36	-31
35	2010.11.30	118.37	39.73	6	3.0	105	40	-58
36	2010.12.12	118.35	39.70	6	3.1	321	86	-50
37	2010.12.18	118.52	39.75	6	2.5	324	55	45
38	2010.12.28	119.33	39.55	9	3.8	309	64	56
39	2011.01.24	118.50	39.68	6	3.4	307	81	-60
40	2011.02.06	117.40	39.78	7	3.5	270	75	0
41	2011.03.07	118.75	39.73	7	3.1	130	89	-10
42	2011.06.12	118.77	39.73	8	2.5	115	45	-36
43	2011.06.15	118.65	39.77	6	2.7	35	47	-69
44	2011.08.19	118.88	39.98	8	2.5	121	40	-82
45	2011.10.19	118.18	39.62	7	2.9	292	48	31
46	2011.10.22	118.72	39.77	6	2.7	294	54	-59
47	2011.11.23	118.87	39.98	6	2.6	296	76	-69
48	2011.11.24	118.47	39.75	6	2.5	25	55	45
49	2011.11.30	118.45	39.75	7	2.5	3	81	-70
50	2011.12.01	117.37	39.82	6	2.8	313	45	45

51	2011.12.12	118.18	39.60	6	3.7	310	82	6
52	2012.02.15	118.65	39.77	5	2.7	255	55	-90
53	2012.02.29	118.48	39.78	6	2.7	305	70	-90
54	2012.04.14	118.23	39.63	6	3.3	359	73	10
55	2012.04.21	118.37	39.73	7	3.2	321	82	50
56	2012.05.22	118.47	39.78	7	2.7	324	56	-72
57	2012.05.24	118.50	39.75	6	3.1	300	46	54
58	2012.05.28	118.47	39.72	22	5.1	322	90	15
59	2012.05.29	118.48	39.78	7	3.7	157	71	-36
60	2012.06.10	117.32	39.38	9	2.8	287	53	-43
61	2012.06.18	117.57	39.62	5	4.5	320	84	8
62	2012.06.20	118.42	39.77	12	2.8	132	85	-65
63	2012.08.26	117.43	39.62	9	4.0	127	84	8
64	2012.09.24	118.52	39.78	6	2.5	131	80	-85
65	2012.11.25	117.63	39.37	8	2.9	84	42	-67
66	2012.12.09	118.85	39.88	7	2.8	335	71	-7
67	2013.01.08	119.22	39.68	6	3.2	314	76	-43
68	2013.01.11	118.82	39.63	6	3.3	320	57	13
69	2013.02.17	118.47	39.78	7	2.9	338	35	-42
70	2013.02.25	118.17	39.57	6	2.8	268	56	-78
71	2013.05.01	118.50	39.77	7	2.7	1	47	69
72	2013.05.03	117.93	39.33	8	2.9	325	85	0
73	2013.06.03	118.50	39.80	6	3.1	330	51	8
74	2013.06.08	118.48	39.77	8	2.5	317	57	-40
75	2013.06.23	118.38	39.72	6	2.8	136	48	-31
76	2013.08.03	118.68	39.78	6	2.8	116	80	-85

77	2013.08.21	118.48	39.97	8	2.6	83	63	-62
78	2013.08.23	118.50	39.93	9	2.6	255	29	-58
79	2013.08.23	118.50	39.93	7	3.2	358	31	-71
80	2014.01.14	118.43	39.75	7	3.4	154	71	24
81	2014.01.25	118.50	39.80	6	3.0	125	52	-27
82	2014.02.11	118.78	39.87	8	2.8	253	36	-54
83	2014.05.10	118.48	39.78	6	2.5	95	66	-33
84	2015.01.11	118.77	39.84	11	3.3	262	57	-140
85	2015.11.15	118.56	39.75	12	3.5	27	70	67
86	2015.11.28	117.93	39.33	15	4.0	60	85	-176
87	2015.12.06	117.92	39.37	23	3.4	47	80	-155
88	2016.02.12	117.95	39.37	14	3.0	67	62	-145
89	2016.03.14	117.95	39.40	19	3.7	204	69	163
90	2016.05.16	118.25	39.64	22	3.5	112	52	-37
91	2017.07.04	118.84	39.31	16	3.1	47	86	-133
92	2017.10.15	118.25	39.63	20	3.1	240	74	-130
93	2017.10.27	118.33	39.70	17	3.4	65	80	-160
94	2018.01.06	118.48	39.67	15	3.4	69	57	-47
95	2018.04.28	118.63	39.65	20	3.2	282	69	-84
96	2018.08.09	119.00	39.94	10	3.5	225	78	-173
97	2018.08.10	118.49	39.79	10	3.1	98	74	7
98	2019.03.09	118.69	40.22	17	3.3	7	72	-167

Table S2. Results of a deterministic geomechanical assessment of fault pore pressure to slip on the mapped faults in Tangshan seismic region in the present ambient stress field.

Name of fault	Segment	Length, km	Delta P_0 to fault slip, MPa
Jiyunhe fault (F_2)	$F_{2\text{-}1}$	25.37	3.70
	$F_{2\text{-}2}$	29.37	14.99
	$F_{2\text{-}3}$	22.25	7.03
Yejituo fault (F_3)	$F_{3\text{-}1}$	32.04	5.47
	$F_{3\text{-}2}$	40.50	5.44
	$F_{3\text{-}3}$	18.69	6.93
	$F_{3\text{-}4}$	12.02	6.15
Tangshan fault belt (F_4)	$F_{4\text{-}1}$	33.38	2.58
	$F_{4\text{-}2}$	18.47	5.95
	$F_{4\text{-}3}$	12.02	2.85
	$F_{4\text{-}4}$	11.57	16.38
	$F_{4\text{-}5}$	11.13	5.40
	$F_{4\text{-}6}$	13.80	2.58
Changli-Ninghe fault (F_5)	$F_{5\text{-}1}$	13.80	5.82
	$F_{5\text{-}2}$	17.80	13.55
	$F_{5\text{-}3}$	13.57	4.93
	$F_{5\text{-}4}$	13.13	3.25
	$F_{5\text{-}5}$	36.05	12.38
	$F_{5\text{-}6}$	18.47	9.22
	$F_{5\text{-}7}$	34.71	5.82
	$F_{5\text{-}8}$	12.91	4.93
	$F_{5\text{-}9}$	27.59	7.41
Lulong fault (F_6)	$F_{6\text{-}1}$	22.92	24.49
	$F_{6\text{-}2}$	19.58	18.04

Luanxian-Laoting fault (F_7)	$F_{7\text{-}1}$	18.25	62.50
	$F_{7\text{-}2}$	6.68	27.03
	$F_{7\text{-}3}$	20.69	7.03
	$F_{7\text{-}4}$	24.03	10.45
	$F_{7\text{-}5}$	17.80	6.00
Baigezhuang fault (F_8)	$F_{8\text{-}1}$	22.70	18.86
	$F_{8\text{-}2}$	8.46	17.80
	$F_{8\text{-}3}$	29.37	10.04
	$F_{8\text{-}4}$	18.25	6.00
Qinbei fault (F_9)	$F_{9\text{-}1}$	41.39	6.39
	$F_{9\text{-}2}$	17.80	5.41
	$F_{9\text{-}3}$	9.79	5.41
Xi'nanzhuang fault (F_{11})	$F_{11\text{-}1}$	20.03	20.56
	$F_{11\text{-}2}$	13.35	7.92
	$F_{11\text{-}3}$	13.35	12.78
Haihe fault (F_{12})	$F_{12\text{-}1}$	18.25	10.70
	$F_{12\text{-}2}$	12.46	6.67
	$F_{12\text{-}3}$	11.13	10.70
	$F_{12\text{-}4}$	33.82	4.90
Hangu fault (F_{13})	$F_{13\text{-}1}$	15.58	4.52
	$F_{13\text{-}2}$	10.68	19.54
	$F_{13\text{-}3}$	11.57	6.19
Cangdong fault (F_{14})	$F_{14\text{-}1}$	25.81	16.89
	$F_{14\text{-}2}$	9.79	10.22
	$F_{14\text{-}3}$	21.81	8.47
Lengkou fault (F_{17})	$F_{17\text{-}1}$	34.27	4.49

$F_{17\text{-}2}$	39.16	4.72
$F_{17\text{-}3}$	20.03	4.54
$F_{17\text{-}4}$	14.24	22.23

Table S3. Probability of fault slip potential on the mapped faults in Tangshan seismic region (beyond a range of 45 km away from the injection wells) in response to the fluid injection at five hypothetic wells in the MTY EGS field.

Name of fault	Segment	Probability of fault slip potential			
		in 2020	in 2030	in 2040	in 2050
Jiyunhe fault (F_2)	$F_{2\text{-}1}$	39%	39%	39%	39%
	$F_{2\text{-}2}$	19%	19%	19%	19%
	$F_{2\text{-}3}$	27%	27%	27%	27%
Yejituo fault (F_3)	$F_{3\text{-}1}$	29%	29%	29%	29%
	$F_{3\text{-}2}$	30%	30%	30%	30%
	$F_{3\text{-}3}$	30%	30%	30%	30%
	$F_{3\text{-}4}$	30%	30%	30%	30%
Tangshan fault belt (F_4)	$F_{4\text{-}1}$	38%	38%	38%	38%
	$F_{4\text{-}2}$	30%	30%	30%	30%
	$F_{4\text{-}3}$	40%	40%	40%	40%
	$F_{4\text{-}4}$	14%	14%	14%	14%
	$F_{4\text{-}5}$	35%	35%	35%	35%
	$F_{4\text{-}6}$	40%	40%	40%	40%
Changli-Ninghe fault (F_5)	$F_{5\text{-}1}$	30%	30%	30%	30%
	$F_{5\text{-}2}$	15%	15%	15%	15%
	$F_{5\text{-}3}$	35%	35%	35%	35%
	$F_{5\text{-}4}$	37%	37%	37%	38%

	$F_{5\text{-}5}$	18%	18%	18%	19%
	$F_{5\text{-}6}$	25%	25%	25%	25%
	$F_{5\text{-}7}$	31%	31%	31%	31%
	$F_{5\text{-}8}$	32%	32%	32%	32%
	$F_{5\text{-}9}$	28%	28%	28%	28%
Lulong fault (F_6)	$F_{6\text{-}1}$	3%	3%	3%	3%
	$F_{6\text{-}2}$	7%	7%	7%	7%
Luanxian-Laoting fault (F_7)	$F_{7\text{-}1}$	1%	1%	1%	1%
	$F_{7\text{-}2}$	4%	4%	4%	4%
	$F_{7\text{-}3}$	30%	30%	30%	30%
	$F_{7\text{-}4}$	26%	26%	26%	27%
	$F_{7\text{-}5}$	32%	32%	33%	33%
Baigezhuang fault (F_8)	$F_{8\text{-}1}$	11%	11%	11%	11%
	$F_{8\text{-}2}$	12%	12%	12%	13%
	$F_{8\text{-}3}$	23%	24%	25%	26%
	$F_{8\text{-}4}$	28%	28%	28%	29%
Qinbei fault (F_9)	$F_{9\text{-}1}$	30%	30%	30%	30%
	$F_{9\text{-}2}$	31%	31%	31%	31%
	$F_{9\text{-}3}$	31%	31%	31%	31%
Xi'nanzhuang fault (F_{11})	$F_{11\text{-}1}$	6%	6%	6%	6%
	$F_{11\text{-}2}$	27%	27%	27%	27%
	$F_{11\text{-}3}$	20%	20%	20%	20%
Haihe fault (F_{12})	$F_{12\text{-}1}$	21%	21%	21%	21%
	$F_{12\text{-}2}$	27%	27%	27%	27%
	$F_{12\text{-}3}$	21%	21%	21%	21%
	$F_{12\text{-}4}$	33%	33%	33%	33%

Hangu fault (F_{13})	$F_{13\text{-}1}$	34%	34%	34%	34%
	$F_{13\text{-}2}$	10%	10%	10%	10%
	$F_{13\text{-}3}$	30%	30%	30%	30%
Cangdong fault (F_{14})	$F_{14\text{-}1}$	7%	7%	7%	7%
	$F_{14\text{-}2}$	17%	17%	17%	17%
	$F_{14\text{-}3}$	20%	20%	20%	20%
Lengkou fault (F_{17})	$F_{17\text{-}1}$	33%	33%	33%	33%
	$F_{17\text{-}2}$	32%	32%	32%	32%
	$F_{17\text{-}3}$	36%	36%	36%	36%
	$F_{17\text{-}4}$	7%	7%	7%	7%

Table S4. Probability of fault slip potential on the boundary faults near the MTY EGS field (within a range of 15 km away from the injection wells) in response to the fluid injection at five hypothetic wells in the MTY EGS field.

Tectonic unit	Segment	Length, km	Probability of fault slip potential			
			in 2020	in 2030	in 2040	in 2050
Between II and I	F_{b1}	3.85	2.0%	2.2%	2.8%	3.6%
	F_{b2}	3.21	0.1%	0.2%	0.3%	0.3%
	F_{b3}	5.64	0.1%	0.1%	0.1%	0.1%
	F_{b4}	1.28	8.1%	14.4%	20.2%	25.0%
	F_{b5}	4.36	14.6%	20.7%	26.5%	30.5%
	F_{b6}	7.56	16.1%	17.3%	20.0%	21.7%
Between II and III	F_{b7}	16.67	35.7%	38.4%	43.9%	47.5%
Between III and IV	F_{b8}	3.08	9.7%	10.3%	11.2%	12.6%
	F_{b9}	3.33	31.0%	32.3%	35.0%	38.1%
	F_{b10}	4.23	12.0%	13.5%	15.8%	18.4%
Between II and IV	F_{b11}	6.15	38.5%	49.2%	55.6%	59.5%

	F_{b12}	3.72	29.5%	46.9%	55.1%	59.7%
	F_{b13}	8.21	11.1%	27.7%	31.5%	35.1%
	F_{b14}	5.77	37.9%	42.9%	49.1%	52.8%
Southwestern II	F_{b15}	4.87	17.4%	18.0%	19.6%	21.6%
Between IV and V	F_{b16}	3.85	8.0%	8.6%	9.3%	10.0%
	F_{b17}	2.69	17.0%	17.9%	19.1%	21.1%
	F_{b18}	9.10	11.3%	12.5%	15.1%	18.0%
	F_{b19}	3.85	37.6%	40.4%	43.4%	46.2%
	F_{b20}	3.08	21.7%	22.6%	24.4%	26.9%

Table S5. The net monthly injection volume used for estimating the maximum magnitude of injection-related earthquakes in the MTY EGS field.

Fluid injected rate, L/s	Monthly injection volume, m^3	Fluid loss	The net injected volume, m^3
1	2.59×10^3		2.59×10^2
10	2.59×10^4		2.59×10^3
20	5.18×10^4		5.18×10^3
30	7.78×10^4		7.78×10^3
40	1.04×10^5		1.04×10^4
50	1.30×10^5		1.30×10^4
60	1.56×10^5	10%	1.56×10^4
70	1.81×10^5		1.81×10^4
80	2.07×10^5		2.07×10^4
90	2.33×10^5		2.33×10^4
100	2.59×10^5		2.59×10^4
110	2.85×10^5		2.85×10^4
120	3.11×10^5		3.11×10^4

1	2.59×10^{3}		5.18×10^{2}
10	2.59×10^{4}		5.18×10^{3}
20	5.18×10^{4}		1.036×10^{4}
30	7.78×10^{4}		1.556×10^{4}
40	1.04×10^{5}		2.08×10^{4}
50	1.30×10^{5}		2.60×10^{4}
60	1.56×10^{5}	20%	3.12×10^{4}
70	1.81×10^{5}		3.62×10^{4}
80	2.07×10^{5}		4.14×10^{4}
90	2.33×10^{5}		4.66×10^{4}
100	2.59×10^{5}		5.18×10^{4}
110	2.85×10^{5}		5.70×10^{4}
120	3.11×10^{5}		6.22×10^{4}
1	2.59×10^{3}		7.77×10^{2}
10	2.59×10^{4}		7.77×10^{3}
20	5.18×10^{4}		1.554×10^{4}
30	7.78×10^{4}		2.334×10^{4}
40	1.04×10^{5}		3.12×10^{4}
50	1.30×10^{5}		3.90×10^{4}
60	1.56×10^{5}	30%	4.68×10^{4}
70	1.81×10^{5}		5.43×10^{4}
80	2.07×10^{5}		6.21×10^{4}
90	2.33×10^{5}		6.99×10^{4}
100	2.59×10^{5}		7.77×10^{4}
110	2.85×10^{5}		8.55×10^{4}
120	3.11×10^{5}		9.33×10^{4}

1	2.59×10^{3}		1.036×10^{3}
10	2.59×10^{4}		1.036×10^{4}
20	5.18×10^{4}		2.072×10^{4}
30	7.78×10^{4}		3.112×10^{4}
40	1.04×10^{5}		4.16×10^{4}
50	1.30×10^{5}		5.20×10^{4}
60	1.56×10^{5}	40%	6.24×10^{4}
70	1.81×10^{5}		7.24×10^{4}
80	2.07×10^{5}		8.28×10^{4}
90	2.33×10^{5}		9.32×10^{4}
100	2.59×10^{5}		1.036×10^{5}
110	2.85×10^{5}		1.140×10^{5}
120	3.11×10^{5}		1.244×10^{5}